

Environmental Science Nano

Accepted Manuscript



This is an *Accepted Manuscript*, which has been through the Royal Society of Chemistry peer review process and has been accepted for publication.

Accepted Manuscripts are published online shortly after acceptance, before technical editing, formatting and proof reading. Using this free service, authors can make their results available to the community, in citable form, before we publish the edited article. We will replace this *Accepted Manuscript* with the edited and formatted *Advance Article* as soon as it is available.

You can find more information about *Accepted Manuscripts* in the [Information for Authors](#).

Please note that technical editing may introduce minor changes to the text and/or graphics, which may alter content. The journal's standard [Terms & Conditions](#) and the [Ethical guidelines](#) still apply. In no event shall the Royal Society of Chemistry be held responsible for any errors or omissions in this *Accepted Manuscript* or any consequences arising from the use of any information it contains.

Nano-Statement

Our study showed that exposure of human lung epithelial cells (BEAS-2B) to multi-walled carbon nanotubes (MWCNTs) with user-defined chemical and physical properties reduces the metabolic activity of mitochondria and induces cell cycle arrest. The analysis also demonstrated that the cellular changes induced upon exposure to MWCNTs could be analyzed by means of atomic force microscopy and nanoindentation, to help provide insights into mechanisms of toxicity and nanomaterial-induced cellular transformation.

Towards Elucidating the Effects of Purified MWCNTs on Human Lung**Epithelial cells**

Chenbo Dong#, Reem Eldawud#, Linda M. Sargent, Michael L. Kashon, David

*Lowry, Yon Rojanasakul, and Cerasela Zoica Dinu**

C. Dong, R. Eldawud, Prof. C. Z. Dinu
Department of Chemical Engineering,
West Virginia University
Morgantown WV, 26506, USA
E-mail: cerasela-zoica.dinu@mail.wvu.edu

Dr. M. L. Kashon, D.L. Lowry, Dr. L. M. Sargent
National Institute for Occupational Safety and Health
Morgantown WV, 26505, USA

Prof. Y. Rojanasakul
Department of Basic Pharmaceutical Sciences
West Virginia University
Morgantown WV, 26506, USA

Equally contributing authors

* Corresponding author

Table of contents entry: Exposure to purified multi-walled carbon nanotubes (MWCNTs) induced cell cycle arrest, reduced mitochondrial activity and changed the cellular biomechanical properties.

Abstract

Toxicity of engineered nanomaterials is associated with their inherent properties, both physical and chemical. Recent studies have shown that exposure to multi-walled carbon nanotubes (MWCNTs) promotes tumors and tumor-associated pathologies and lead to carcinogenesis in model *in vivo* systems. Herein we examined the potential of purified MWCNTs used at occupationally relevant exposure doses for particles not otherwise regulated to affect human lung epithelial cells. The uptake of the purified MWCNTs was evaluated using fluorescence activated cell sorting (FACS), while the effects on cell fate were assessed using 2- (4-iodophenyl) - 3- (4-nitrophenyl) - 5-(2,4-disulfophenyl) -2H-tetrazolium salt colorimetric assay, cell cycle and nanoindentation. Our results showed that exposure to MWCNTs reduced cell metabolic activity and induced cell cycle arrest. Our analysis further emphasized that MWCNTs-induced cellular fate results from multiple types of interactions that could be analyzed by means of intracellular biomechanical changes and are pivotal in understanding the underlying MWCNTs-induced cell transformation.

Keywords: Carbon nanotubes, cyto-genotoxic effects, cell cycle arrest, biomechanical changes

1. Introduction

Multi-walled carbon nanotubes (MWCNTs) aspect-ratio and their ease of functionalization with drugs and biomolecules were recently shown to increase their cellular delivery for applications in diagnostics,¹ drug delivery² and cancer therapies.³ ⁴ Studies also showed that dispersion stability and loading conditions could influence MWCNTs-induced therapeutic effects as well as the efficiency of a loaded drug.⁵ However, such studies failed to reduce the MWCNTs-induced inflammatory effects ⁶ or to resolve the overall mechanisms of toxicity associated with MWCNTs cellular uptake. ⁷⁻¹⁰

Purification via strong acids oxidation was recently used as a mean to increase nanotube dispersity and modify both their chemical and physical properties.¹¹ Strong acid oxidation shortened the MWCNTs by cutting them at their defect sites, removing impurities and inducing O-derivated functionalities.¹² Such purified MWCNTs had lower immunological toxicity on BALB/c mice when compared to their impure counterparts (i.e, MWCNTs containing Fe on their external or internal walls).¹³ Complementary, shorter MWCNTs were shown to illicit reduced inflammatory and toxicity responses in the pleural cavity of the mice.¹⁴ Further, exposure to shorter and purified MWCNTs was shown to lead to changes in the mechanical properties of epithelial cells ¹⁵ used previously as models for nanomaterial assessment.⁸ However, it is still subject to debate to what extent such purified forms of MWCNTs influence cell fate and what are the resulting nanotube-induced cell transformations that could lead to toxicity and cancer development. Failure to assess such effects could potentially jeopardize the implementation of the purified forms in MWCNTs-based

nanotherapeutics.¹⁶

Combining conventional biocellular and nanoindentation assays¹⁵ we proposed to unravel the cellular changes induced by exposure to purified MWCNTs, all as a function of the nanomaterial physical and chemical properties. Since the respiratory tract is the primary route of exposure by inhalation,¹⁷ lung-derived BEAS-2B cells were considered a suitable model system to evaluate MWCNTs-induced cellular changes^{8, 15} with the exposure dose being determined by extrapolation of *in vivo* studies mimicking human exposure for 20 weeks at Occupational Safety and Health Administration (OSHA) permissible limits for particles not otherwise regulated.⁸

2. Materials and Methods

2.1 Multi-walled carbon nanotubes (MWCNTs) purification

MWCNTs (Nanolab Inc., 100 mg) were purified by ultrasonication (Branson 2510, Fisher Scientific) in a strong mixture of sulfuric (Fisher Scientific, 96.4%) and nitric (Fisher Scientific, 69.5%) acids (volume ratio 3:1) for 1 h at a temperature of about 23°C. Upon time elapsed, the mixture was diluted in deionized water (DI water) and filtered through a polycarbonate membrane (Fisher Scientific, GTTP 0.2 μm); the process was repeated several times to remove acid residues or impurities. Purified MWCNTs were collected on a fresh GTTP filter, dried, and stored at room temperature.

2.2 MWCNTs characterization

Fourier Transform Infrared Spectroscopy (FTIR, Digilab FTS 7000) equipped with diamond Attenuated Total Reflection (ATR) crystal was used to investigate the chemical properties of pristine and purified MWCNTs. Scans ranging from 1000 to 4000 cm^{-1} were collected.

Morphology and elemental quantitative analyses of pristine and purified MWCNTs (1 mg/mL sample on silica wafer) were performed on a Hitachi S-4700 Field Emission Scanning Electron Microscope (Hitachi High-Technologies Corporation) containing a S-4700 detector combining secondary (SE) and backscattered (BSE) electron detection and operating at 20 KV. For Energy Dispersive X-Ray Spectroscopy (EDX) results are shown as weight percent of a given

element relative to the most dominant element present in the sample.

The average length distribution of the pristine and purified MWCNTs was evaluated using tapping mode Atomic Force Microscopy (AFM) performed in air (Asylum Research, AC240TS, 50 to 90 kHz). At least 3 scans of $10\ \mu\text{m} \times 10\ \mu\text{m}$ were acquired for each of the sample being analyzed and a minimum of 30 individual MWCNTs were measured to obtain an average length distribution.

2.3 Functionalization of MWCNTs with fluorescent protein

Alexa 488-labeled Bovine Serum Albumin or Bovine Serum Albumin (Alexa-BSA, or BSA, Invitrogen) was covalently attached to purified MWCNTs using 1-ethyl-3-[3-dimethylaminopropyl] carbodiimide hydrochloride (EDC, Acros Organics) and N-hydroxysuccinimide (NHS, Pierce) chemistry.¹⁸ Briefly, 2 mg of purified MWCNTs were dispersed in 160 mM EDC and 80 mM NHS (total volume of 2 mL in 2-(N-morpholino) ethanesulfonic acid sodium salt or MES, 50 mM, pH 4.7, (Sigma) for 15 min at room temperature with shaking at 200 rpm. EDC/NHS activated MWCNTs were subsequently filtered through a GTTP filter membrane, washed thoroughly with MES buffer, and immediately re-dispersed in 2 mL of 1 mg/mL protein solution in Phosphate Saline Buffer (PBS, Fisher), 100 mM, pH 7.4. The mixture was incubated for 3 h at room temperature with shaking at 200 rpm. Upon incubation, the resulting protein-based conjugates were filtered and washed extensively with PBS to remove any unbound protein. The supernatant and the first two washes were collected.

2.4 Protein loading

The amount of protein bound onto the purified MWCNTs (i.e., protein loading) was determined using standard bicinchoninic acid assay (BCA, Fisher).¹⁸ For this, the working reagent was prepared by mixing 50 parts of reagent A (1000 μ L), with 1 part of reagent B (50 μ L) and subsequently mixing 1000 μ l of that working reagent with 50 μ L of either the collected supernatant or washes. The resulting solution was gently vortexed and incubated in a water bath at 37°C for 30 min. Upon time elapsed, the absorbance values were recorded on a Spectrophotometer (Evolution 300/600, Thermo Fisher) using 562 nm as reading wavelength. Control calibration curves were prepared using serial dilutions of protein in the working buffer. The relative amount of Alexa-BSA bound to the purified MWCNTs was estimated from the difference between the amount of protein initially added during the covalent incubation step and the amount of the protein removed in the supernatant and two washes as calculated by the BCA assay.

2.5 Dispersity analysis

The dispersity of MWCNTs or MWCNTs-functionalized with the protein was tested both in DI water and in Dulbecco's Modified Eagle Media (DMEM, Invitrogen) containing 10% Fetal Bovine Serum (FBS, Invitrogen). For this, MWCNTs were sonicated in the testing solution (for a final concentration of 5 mg/mL) and subsequently centrifuged at 3000 rpm for 5 min. Part of the corresponding supernatant (0.8 mL) was collected, filtered through a 0.2 μ m GTPP filter membrane and then

dried under vacuum. The amount of MWCNTs isolated on the filter was weighted and the dispersity was determined relative to the starting amount and volume used per individual sample.

2.6 Cell culture

Immortalized human bronchial epithelial cells (BEAS-2B, ATCC) were cultured in DMEM media containing 10% FBS, 0.1% L-glutamine and 1% penicillin/streptomycin (Invitrogen). Cells were maintained in a humidified atmosphere at 37°C and with 5% CO₂; for passaging, a 0.25% trypsin (Invitrogen) solution was used.

2.7 Fluorescence Activated Cell Sorting (FACS)

BEAS-2B cells were seeded for 24 h in T75 flasks (Fisher) at a density of 3.71×10^5 cells. Subsequently, the cells were exposed to $24 \mu\text{g}/\text{cm}^2$ Alexa-BSA-MWCNTs conjugates dispersed in fresh media by brief sonication. Control samples, i.e., cells exposed to PBS, free Alexa-BSA at the equivalent amount to the Alexa-BSA amount loaded onto the MWCNTs, and cells exposed to unlabeled MWCNTs respectively, were performed in parallel. Upon 24 h incubation, the cells in each treatment group were washed with PBS, trypsinized (0.25% trypsin/EDTA, Fisher), suspended in DMEM containing 10% FBS and centrifuged at 1200 rpm for 5 min to remove free proteins, non-internalized, loosely bound nanotubes or conjugates. Upon centrifugation the samples were washed with PBS, fixed with 100 μL of 4%

glutaraldehyde solution (Fisher) for 15 min at room temperature, and then extensively washed with PBS to remove free glutaraldehyde.

Analyses were performed on a FACS Caliber flow cytometer (Becton Dickinson). The forward scatter (FSC) and side scatter (SSC) were used to gate the samples to exclude the cellular debris. FITC signal for the BSA-based conjugates used 488 nm excitation and 515 nm emission wavelengths. At least 30000 events were recorded for each sample and the data was analyzed and plotted using FlowJo v7.2.5 software.

2.8 Cell activity

BEAS-2B cells were seeded overnight at a density of 1.5×10^4 into a 96-well plate (Fisher) and exposed for 24, 48 and 72 h respectively to $24 \mu\text{g}/\text{cm}^2$ purified MWCNTs dispersed by brief sonication in the culture media. Upon time elapse, 10 μl of tetrazolium salt (i.e., 2-(4-iodophenyl) - 3-(4-nitrophenyl) - 5-(2,4-disulfophenyl) - 2H-tetrazolium also known as WST-1, Roche), was added to each well and the plate was incubated for 2 h at room temperature. Changes in the color of the individual wells were based on the cells ability to cleave WST-1 salt to farmazan in the presence of the enzyme dehydrogenase and were assessed using a BioTek 96 plate reader (BioTek) and 450 nm absorbance. The changes are reported as percentage relative activity of exposed versus unexposed cells.

2.9 Cell cycle analysis

BEAS-2B cells were seeded overnight in 6 well plates (Fisher) at a concentration of 3×10^5 cells/well, and exposed for 24 h to $24 \mu\text{g}/\text{cm}^2$ purified MWCNTs dispersed in cellular media. Following exposure to MWCNTs, cells were trypsinized, collected, washed twice with PBS, centrifuged at 1500 rpm for 6 min and fixed overnight in 2 mL 70% ethanol (Fisher) at -20°C . Subsequently, the cells were washed again, suspended in 0.2% Tween 20 (Sigma Chemicals) for 15 min, treated with $10 \mu\text{l}$ 0.05% RNase for 15 min and stained with $30 \mu\text{l}$ propidium iodide (Sigma). Changes in DNA content were determined using BD LSR Fortessa Flow cell analyzer (BD Biosciences), and the BD FACS Diva (Verity Software House) and FlowJo V10.0.7 (Tree Star Inc.) software. The forward scatter (FSC) and side scatter (SSC) were used to gate the majority of the cell population; 20000 events were collected for each sample. The selection of the cells was based on knowing that in the G₀/G₁ phase (before DNA synthesis) cells have a defined amount of DNA (i.e., a diploid chromosomal DNA content) and double that amount in G₂ or M phases (G₂/M, i.e., a tetraploid chromosomal DNA content). Complementary, during the S phase (DNA synthesis), cells contain between one to two DNA levels.

2.10 Cell nanomechanical properties analysis

BEAS-2B cells were seeded overnight in 50 mm x 9 mm parallel culture Petri dishes (BD Biosciences) at a density of 1×10^5 cells per dish. Cells were exposed to $24 \mu\text{g}/\text{cm}^2$ purified MWCNTs for 24 h. MFP-3D-BIO AFM (Asylum Research,

TE2000-U) was used to evaluate individual cell Young modulus. Individual cells were selected using optical microscopy and scanned in contact mode in liquid using an Olympus TR400-PB cantilever; the spring constant of the cantilever was measured before each experiment by using a thermal tuning method.¹⁹ The trigger force was in the nanonewtons range (i.e., 2.3-4.0 nN) while the fitting percentage considered for the data analysis was 90%. Analysis was based on the Sneddon's modification of the Hertz model for a four-sided pyramid^{20,21} with the stiffness being calculated knowing the indentation of the tip and the Poisson's ratio of the cell ($\nu=0.5$).²¹

2.10 Statistical analysis

For the FTIR, the experiments were repeated at least three times each with two replicates for a total of 6 replicates.

Statistical analyses for the biomechanical and cell cycle experiments were performed with SAS/STAT software (v9.2) for Windows.

Two-way analysis of variance (ANOVA) and unpaired two-tailed Student's t-test by SigmaPlot 10.0 (Systat Software Inc.) were used to study the effects of MWCNTs on cellular activity and the BSA loading. Experiments were repeated at least three times each with three replicates for a total of 9 replicates.

Differences were considered significant for $p^* < 0.05$.

3. Results and Discussion

MWCNTs purification in sulfuric/nitric acids mixture²² was used to eliminate possible catalyst precursors otherwise present during the nanotube synthesis.¹¹ Pristine and purified MWCNTs samples were investigated using Scanning Electron Microscopy (SEM), Atomic Force Microscopy (AFM), Attenuated Total Reflection Fourier Transform Infrared Spectroscopy (ATR-FTIR), and Energy Dispersive X-ray spectroscopy (EDX) spectroscopy for their physical and chemical properties. SEM analysis showed that purification did not significantly change the morphology of the MWCNTs (Figure S1), while AFM analysis showed that the average length of the purified MWCNTs (792 ± 254 nm) was about 81% shorter than that of pristine MWCNTs (4261 ± 2354 nm; Table S1), which is consistent with previous reports.¹¹

Research has shown that shortening of the MWCNTs leads to formation of chemical groups such as COOH,²³ OH,²⁴ and CO¹² at the nanotube defect sites. Our ATR-FTIR analysis confirmed the presence of the O-containing functional groups (Figure 1a). The peak at 3370 cm^{-1} was attributed to the O-H stretching vibration²⁵ while the peak around 1670 cm^{-1} was associated with the C=O stretching vibration.²⁶ In addition, the small peak at around 1330 cm^{-1} was a result of the O-H bending vibration,²⁷ and the wide range of peaks between $1000\text{-}1250 \text{ cm}^{-1}$ were associated with the C-O stretching vibrations.²⁸ The peak around 2000 cm^{-1} was previously associated with MWCNTs functionalization with O-containing groups.^{29, 30} The increase in O-containing functional groups and removal of metal catalysts was confirmed by EDX (Table S2), with the analysis also showing a decrease in the Fe

and Cu contents for the purified MWCNTs relative to their pristine counterparts.¹¹

The solubility of pristine, purified and protein-MWCNTs conjugates was also tested; well-dispersed MWCNTs are required to eliminate mass transfer limitations when studying the interactions of such nanomaterials with cellular systems.^{31, 32} Analysis showed that purified MWCNTs were highly dispersed, especially in DMEM media (Table S3), presumably due to the: (1) formation of carboxylate anions, and/or (2) the hydrodynamic size of the purified nanotube. For the first, the negative charges or the carboxylate anions resulted upon nanotube treatment with the acids mixture could potentially lead to strong electrostatic repulsion between individual MWCNTs,^{33, 34} while the presence of proteins and amino acids in the DMEM media can aid to the increased dispersity.³⁵ For the second, the shorter nanotubes (as shown by AFM) have smaller hydrodynamic radius and thus end-to-end distances than their pristine counterparts.³⁶

Human bronchial respiratory epithelial cells (BEAS-2B) were exposed to 24 $\mu\text{g}/\text{cm}^2$ of purified MWCNTs covalently functionalized with Alexa-BSA for 24 h; uptake of fluorescently labeled MWCNTs was evaluated as a change in the forward scatter (FSC) and side scatter (SSC) of the exposed cells by using a Fluorescence Assisted Cell Sorting (FACS) machine. Cells exposed to purified MWCNTs alone, cells exposed to free Alexa-BSA, and cells exposed to media were used as controls. Figure 1b shows a significantly higher FITC signal for cells treated with Alexa-BSA-MWCNTs conjugates relative to all the control experiments. The higher signal was consistent with internalization of the labeled MWCNTs, with the relatively lower

intensity observed for the cells exposed to free Alexa-BSA presumably due to the increased Alexa-BSA susceptibility for proteasomal degradation upon its uptake relatively to the more stable MWCNTs-immobilized Alexa-BSA.³⁷⁻³⁹

To investigate the cellular activity upon uptake of MWCNTs, the exposed cells were assessed using WST-1 assay to measure the mitochondrial dehydrogenase activity (Figure 1c). Mitochondria are relatively sensitive organelles known to respond to cellular stresses caused by the uptake of CNTs.⁴⁰ WST-1 was preferred to the MTT assay due to existing concerns regarding CNTs interaction with the nonsoluble tetrazolium salt formed in the later.⁴¹ Our results showed a significant reduction in the cellular activity of the cells exposed for 24, 48, and 72 h to the purified MWCNTs. The reduction was presumably due to the internalized MWCNTs initiating mitochondrion stress that could have led to increased concentrations of cytoplasmic (Ca^{2+})⁴² and changes in the mitochondrial permeability transition membrane pores (MPTPs) potential.⁴³ Studies have shown that when MPTPs are open, the cytochrome Ca^{2+} pro-apoptotic factor (located in the inner membrane of the mitochondria) and Ca^{2+} diffuse into the mitochondrial matrix and could trigger caspases-8 -9 and -3 signaling eventually leading to cell apoptosis.^{42, 44}

Changes in the cellular activity observed upon exposure to purified MWCNTs were further translated into changes in the cell cycle progression,⁴⁵ Figure 2 shows cell cycle arrest at the G1/S phase 24 h post-exposure. Specifically, gating of the cell population (Figure 2a) or single cells (Figure 2b) showed that cells exposed to purified MWCNTs had a statistically significant increase in G1 (gap) phase

($13 \pm 5.35\%$) and a significant decrease in S (synthesis) phase ($25 \pm 6.42\%$; Figure 2d), both relative to controls ($p < 0.05$; Figure 2c) (Table S4). The increase in G1 could be associated with an extensive change in the DNA content, cell volume, and/or increased synthesis of mRNA and proteins.⁴⁶ The change in the S phase could be associated with a decrease of available cellular DNA⁴⁷ based on the known affinity of CNTs for nuclei acids.⁴⁸ The observed changes in the cell cycle progression could lead to defects in DNA synthesis and chromosome segregation and hint to the possibility of MWCNTs to induce genotoxicity⁸ thus complementing previous reports showing CNT-induced chromosomal damage,⁴⁹ generation of reactive oxygen species (ROS),⁵⁰ or multipolar mitotic spindles.^{8, 51}

Changes in the cellular activity and cell cycle progression were complemented by changes in the cell biomechanics (Figure 3). Previous studies have shown that changes in cellular biomechanics with an increase in cell deformability correlate with the progression of a cell to a transformed phenotype, i.e., from a benign to a malignant one.⁵² Further, previous research showed that the AFM can be used to investigate biomechanical properties of fixed cells treated with MWCNTs¹⁵ or to identify cancer cells from a mixture with normal cells,⁵³ with reports showing that for an applied force above 7 nN the elastic modulus of a single cell is relatively independent of the tip indentation.⁵⁴

The elastic modulus distributions of control and MWCNTs-exposed live cells (both cell bodies and cell nuclei) are shown in Table 1, with a typical example of force-indentation (F-Z) curve recorded at the nucleus region shown in Figure 3a.

Compared to the control cells, the cells exposed to purified MWCNTs showed less deformation suggesting a change in their elastic properties, especially at their nuclear regions where the engaging of the AFM tip was weaker than at the cell edges typically consisting concentrated cytoskeleton fibers.⁵⁵ Comparison between the elastic modulus of purified MWCNTs-exposed live cells and control live cells showed a relatively narrow Young modulus distribution for their nucleus regions (0-6kPa) and a much wider distribution for the whole cell bodies (0-12kPa); higher elastic modulus (~20 kPa) was observed at the cell periphery and was attributed to the effects induced by the plastic substrate.⁵⁶ Specifically, the average Young moduli for the whole cell bodies were 2.72 ± 0.96 and 3.84 ± 1.12 kPa for control and exposed live cells respectively, while the average Young moduli at their nuclei regions were 1.58 ± 0.67 and 2.20 ± 0.59 kPa respectively (Figure 3b).

Based on the observed live cell changes, we propose that cellular uptake of the purified MWCNTs induces a series of concurrent processes (i.e., changes in cellular activity and biomechanical properties), which are function of the nanomaterial physical and chemical properties. Such changes could possibly induce cytoskeletal filament reorganization which could lead to increased cellular rigidity, and possible inhibition and/or blockage of intracellular biomolecular transport or cell cycle progression (Figure 4). Preliminary research has shown that exposure to MWCNTs led to their cellular integration either into the endosomal structures⁵⁷ or into cytoskeletal filaments⁵¹ leading to the formation of hybrid-MWCNTs filaments.^{8, 15} Interestingly, the elastic moduli for control BEAS-2B cells were higher than

previously reported (~75%)⁵⁵ presumably due to variation in the cell culture⁵⁸ or nanoindentation and fixation conditions.⁵⁴ Our data supports recent evidence that relates MWCNTs cytotoxic and genotoxic effects to both their physical and chemical properties⁵⁹ and suggests that occupational exposure to such nanomaterials needs to be fully assessed before implementation in biomedical-related applications is sought.

4. Conclusions

Our results showed that purified MWCNTs exposure affects the mitochondrial activity, cell biomechanical properties and cell cycle progression in human lung epithelial cells. The analysis further hints at a possible cyto and genotoxic synergism associated with the cellular exposure to MWCNTs which could potentially induce cell transformation and thus cancer progression.

Author contribution

C.D and R.E have performed the vast majority of the experiments and drafted the manuscript. D.L. performed the cellular exposure to MWCNTs for the elasticity analysis; L.M.S has supervised these experiments. M.L.K. has performed the cell cycle and cell elasticity statistical analysis. Y.R. provided guidance in the design of the cell activity assays. C.Z.D has designed the experiments and finalized the manuscript. All authors have approved the manuscript.

Acknowledgements

Support for this research was provided through NanoSAFE, National Science Foundation grant EPS-1003907, NORA 927000Y and the National Institute of Health (NIH; R01-ES022968).

Authors acknowledge the use of the WVU Shared Research Facilities and the help of Jeremy Hardinger with EDX analysis. Flow cytometry experiments were performed in the Flow Cytometry Core Facility at WVU; the core is in part supported by the National Institute of Health equipment grant number S10OD016165 and the Institutional Development Award (IDeA) from the National Institute of General Medical Sciences of the National Institutes of Health under grant numbers P30GM103488 (CoBRE) and P20GM103434 (INBRE). The authors acknowledge the support and expertise of Dr. Karen Martin, the director of the Core Facility.

Conflict of Interests

Research findings and conclusions are those of the authors and do not necessarily represent the views of the National Institute for Occupational Safety and Health. The authors declare no competing financial interest.

Figure caption

Figure 1: (a) FTIR spectrum of pristine MWCNTs and purified MWCNTs (n=6). (b) FITC intensity of control cells, purified MWCNTs, BEAS-2B cells treated with Alexa-BSA and cells treated with Alexa-BSA-MWCNTs conjugates (n=9). (c) (%) Changes in the activity of the cells exposed to 24 $\mu\text{g}/\text{cm}^2$ purified MWCNTs. Changes are considered significant for $p^* < 0.05$.

Figure 2: Fluorescence Activated Cell Sorting (FACS) was used to evaluate the changes in cell cycle upon exposure to purified MWCNTs; PI-stained BEAS-2B cells were used. (a) Forward scatter (FSC) and side scatter (SSC) 2D-plot showing a representative gating of the live cell population. (b) Scatter plot selection of single cells; representative gating. (c) Cell cycle analysis of controls cell and (d) cells exposed to purified MWCNTs respectively.

Figure 3: (a) Schematic diagram of the force-indentation profile of control and cell exposed to purified MWCNTs. The red curve follows the approach of the tip to the plastic surface while the blue curve follows the detachment of the tip from the surface. “*” indicates the point at which the tip deflected from the surface to allow acquisition of the force-indentation measurement profile. (b) Average Young modulus of the whole live cell and the nucleus region of control and live cells exposed to purified MWCNTs for 24 h. All differences were considered statistically significant for $p^* < 0.05$.

Figure 4: Exposure to purified MWCNTs induced cyto-genotoxic effects by reducing cellular activity, changing cell's biomechanical properties and disrupting the cell cycle.

Table 1: Young's modulus distribution of control live cells and live cells exposed to purified MWCNTs.

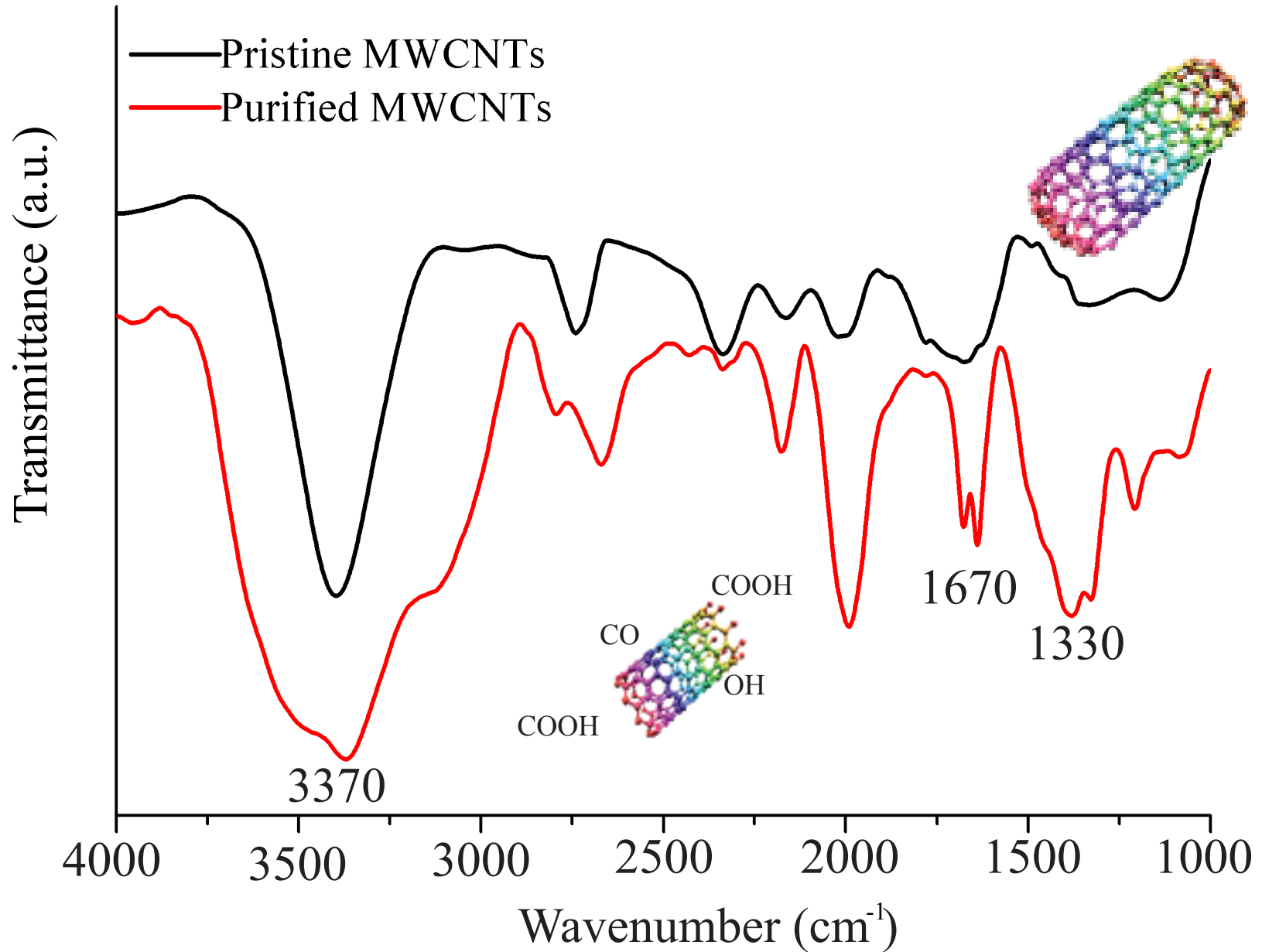
Group	Counts	0-2kPa	2-4kPa	4-6kPa	6-10kPa	>10kPa
Control (whole cells)	380	50.79%	31.84%	10.79%	6.05%	0.53%
Cells incubated with purified MWCNTs (whole cells)	475	37.89%	35.58%	14.32%	7.79%	0.62%
Control (nucleus region)	104	76.92%	21.53%	1.55%	0%	0%
Cells incubated with purified MWCNTs (nucleus region)	122	57.38%	30.07%	12.55%	0%	0%

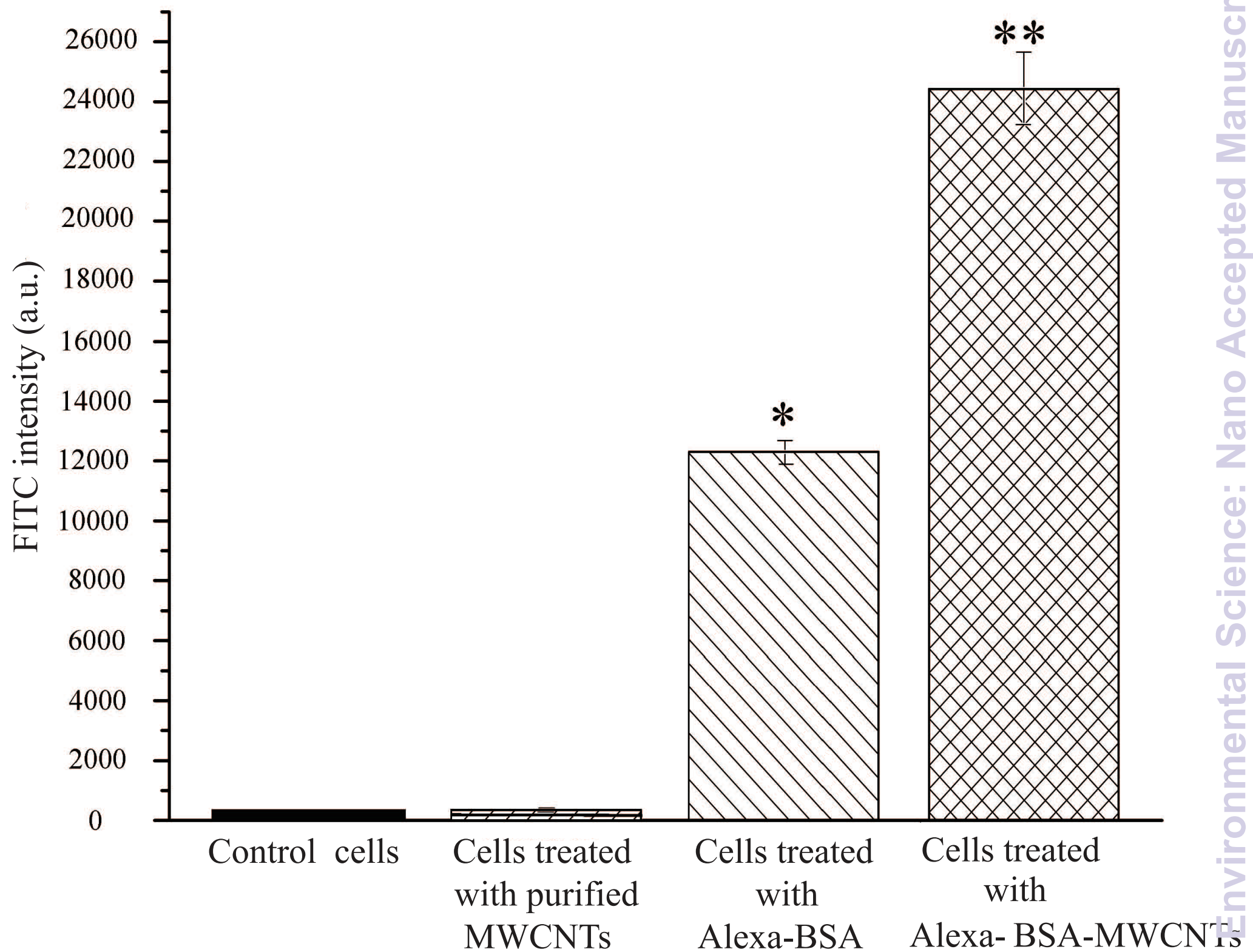
References

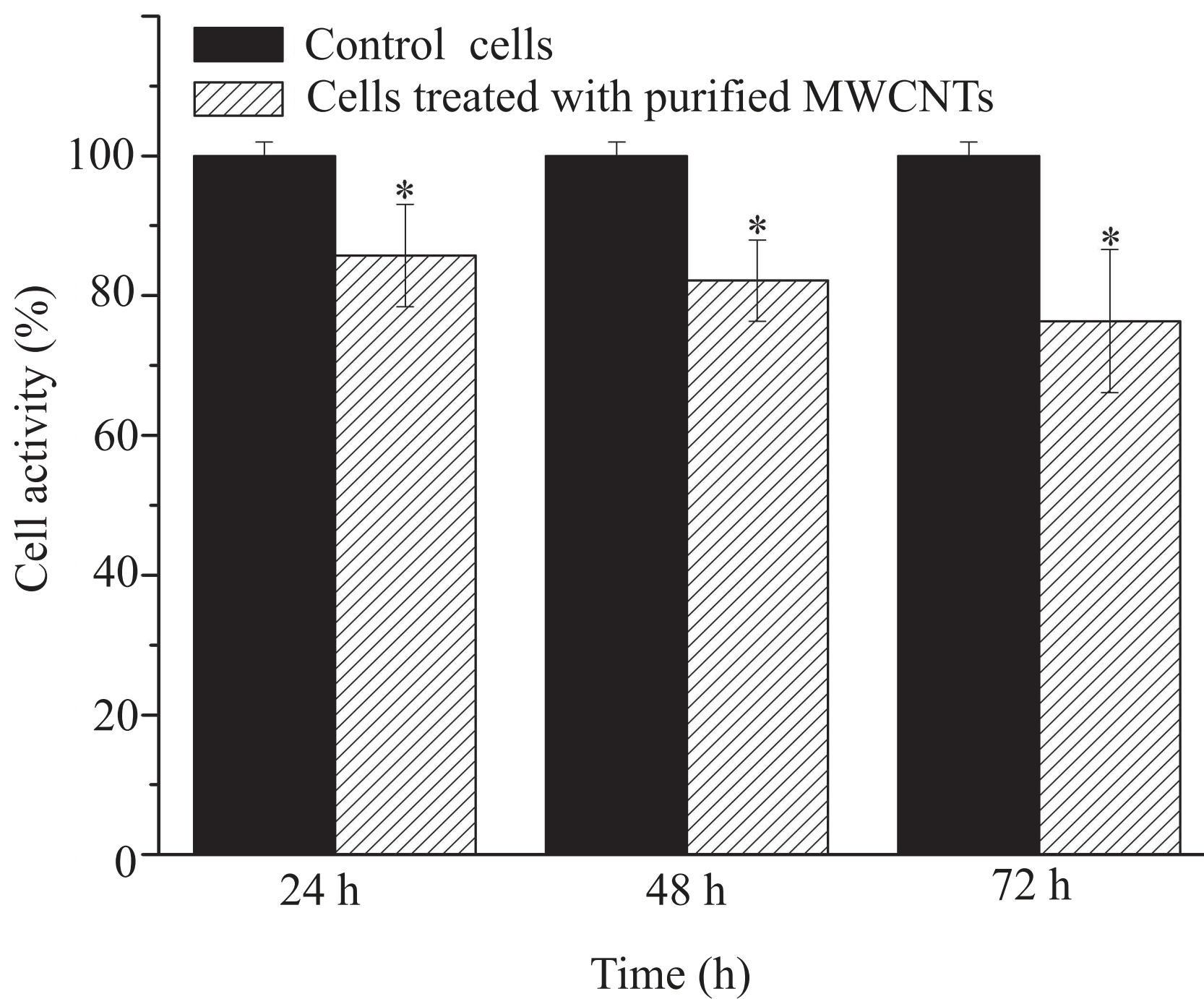
1. L. G. Delogu, G. Vidili, E. Venturelli, C. Menard-Moyon, M. A. Zoroddu, G. Pilo, P. Nicolussi, C. Ligios, D. Bedognetti, F. Sgarrella, R. Manetti and A. Bianco, *P. Natl. Acad. Sci. USA*, 2012, **109**, 16612-16617.
2. M. Das, R. P. Singh, S. R. Datir and S. Jain, *Mol. Pharmaceut.*, 2013, **10**, 3404-3416.
3. H. C. Tsai, J. Y. Lin, F. Maryani, C. C. Huang and T. Imae, *Int. J. Nanomed.*, 2013, **8**, 4427-4440.
4. J. Li, A. Pant, C. F. Chin, W. H. Ang, C. Menard-Moyon, T. R. Nayak, D. Gibson, S. Ramaprabhu, T. Panczyk, A. Bianco and G. Pastorn, *Nanomedicine-Uk*, 2014, in press
5. L. Jiang, T. B. Liu, H. He, L. A. Pham-Huy, L. L. Li, C. Pham-Huy and D. L. Xiao, *J. Nanosci. Nanotechnol.*, 2012, **12**, 7271-7279.
6. T. M. Sager, M. W. Wolfarth, M. Andrew, A. Hubbs, S. Friend, T. H. Chen, D. W. Porter, N. Q. Wu, F. Yang, R. F. Hamilton and A. Holian, *Nanotoxicology*, 2014, **8**, 317-327.
7. E. M. Aneta Fraczek-Szczypta, Tahmina Bahar Syeda, Anil Misra, Mohammad Alavijeh, Jimi Adu, Stanislaw Blazewicz, *J. Nanopart. Res.*, 2012, **14**, 1181-1-1181-14.
8. K. J. Siegrist, S. H. Reynolds, M. L. Kashon, D. T. Lowry, C. B. Dong, A. F. Hubbs, S. H. Young, J. L. Salisbury, D. W. Porter, S. A. Benkovic, M. McCawley, M. J. Keane, J. T. Mastovich, K. L. Bunker, L. G. Cena, M. C. Sparrow, J. L. Sturgeon, C. Z. Dinu and L. M. Sargent, *Part. Fibre. Toxicol.*, 2014, **11**, 1-15.
9. M. Pacurari, X. J. Yin, M. Ding, S. S. Leonard, D. Schwegler-Berry, B. S. Ducatman, M. Chirila, M. Endo, V. Castranova and V. Vallyathan, *Nanotoxicology*, 2008, **2**, 155-170.
10. A. Erdely, M. Dahm, B. T. Chen, P. C. Zeidler-Erdely, J. E. Fernback, M. E. Birch, D. E. Evans, M. L. Kashon, J. A. Deddens, T. Hulderman, S. A. Bilgesu, L. Battelli, D. Schwegler-Berry, H. D. Leonard, W. McKinney, D. G. Frazer, J. M. Antonini, D. W. Porter, V. Castranova and M. K. Schubauer-Berigan, *Part. Fibre. Toxicol.*, 2013, **10**, 1-14.
11. C. B. Dong, A. S. Campell, R. Eldawud, G. Perhinschi, Y. Rojanasakul and C. Z. Dinu, *Appl. Surf. Sci.*, 2013, **264**, 261-268.
12. H. O. Rike Yudianti, Yukie Saito, Tadahisa Iwata, Jun-ichi Azuma, *Open Mater. Sci.* 2011, **5**, 242-247.
13. S. Koyama, Y. A. Kim, T. Hayashi, K. Takeuchi, C. Fujii, N. Kuroiwa, H. Koyama, T. Tsukahara and M. Endo, *Carbon*, 2009, **47**, 1365-1372.
14. F. A. Murphy, A. Schinwald, C. A. Poland and K. Donaldson, *Part. Fibre. Toxicol.*, 2012, **9**, 1-15.
15. C. B. Dong, M. L. Kashon, D. Lowry, J. S. Dordick, S. H. Reynolds, Y. Rojanasakul, L. M. Sargent and C. Z. Dinu, *Adv. Healthcare Mater.*, 2013, **2**, 945-951.

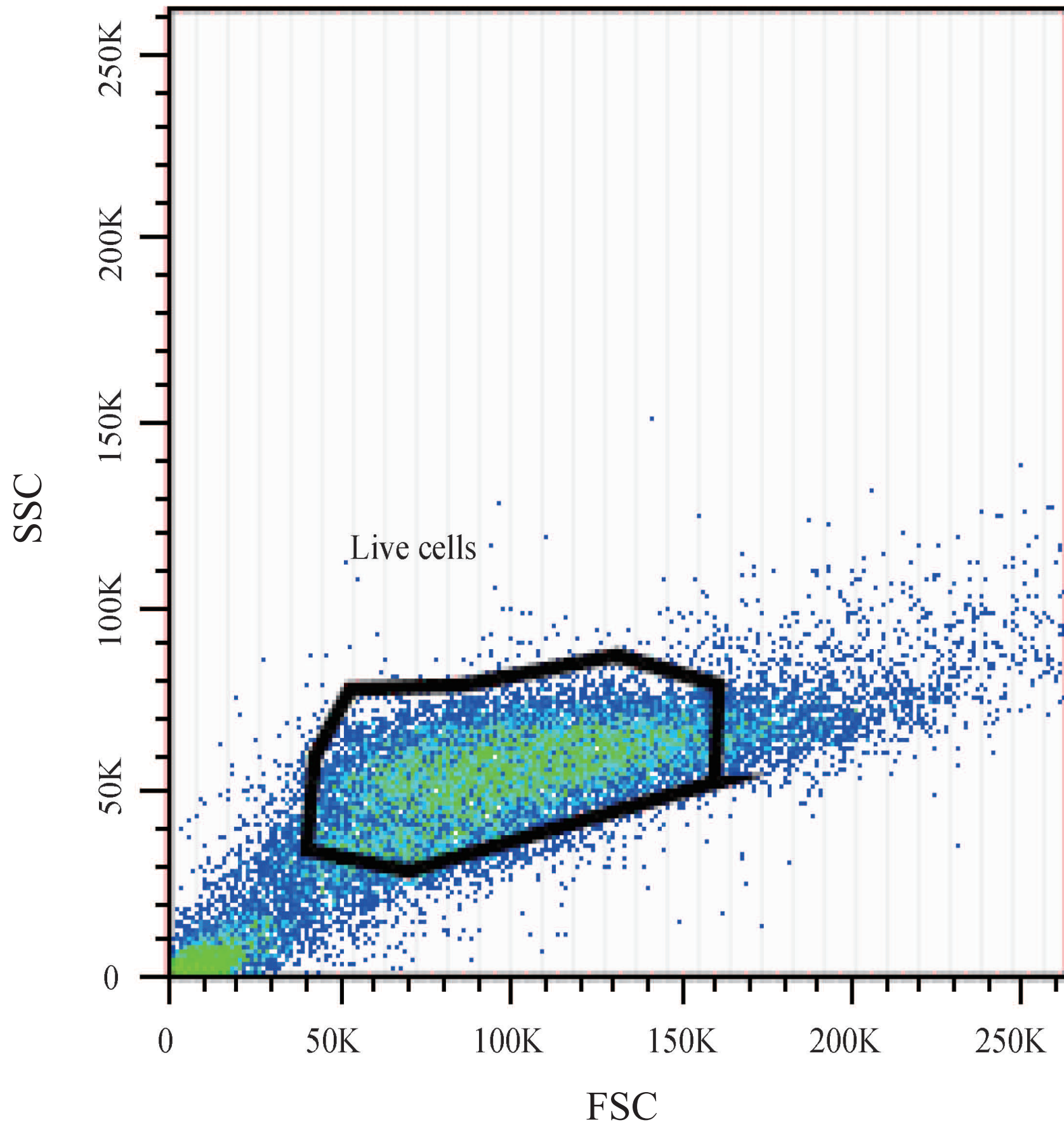
16. G. M. Rogers-Nieman and C. Z. Dinu, *Wiley Interdiscip. Rev. Nanomed. Nanobiotechnol.*, 2014, **6**, 327-337.
17. R. R. Mercer, J. F. Scabilloni, A. F. Hubbs, L. A. Battelli, W. McKinney, S. Friend, M. G. Wolfarth, M. Andrew, V. Castranova and D. W. Porter, *Part. Fibre. Toxicol.*, 2013, **10**, 2-11.
18. A. S. Campbell, C. Dong, F. Meng, J. Hardinger, G. Perhinschi, N. Wu and C. Z. Dinu, *ACS. Appl. Mater. Interfaces*, 2014, **6**, 5393-5403.
19. B. Ohler, *Rev Sci Instrum*, 2007, **78**, 063701-1-063701-5.
20. C. Rotsch, K. Jacobson and M. Radmacher, *P. Natl. Acad. Sci. USA*, 1999, **96**, 921-926.
21. M. Radmacher, M. Fritz, C. M. Kacher, J. P. Cleveland and P. K. Hansma, *Biophys. J.*, 1996, **70**, 556-567.
22. B. Scheibe, E. Borowiak-Palen and R. J. Kalenczuk, *Mater. Charact.*, 2010, **61**, 185-191.
23. V. Datsyuk, M. Kalyva, K. Papagelis, J. Parthenios, D. Tasis, A. Siokou, I. Kallitsis and C. Galiotis, *Carbon*, 2008, **46**, 833-840.
24. Z. H. Qu and G. J. Wang, *J. Nanosci. Nanotechnol.*, 2012, **12**, 105-111.
25. B. P. Singh, D. Singh, R. B. Mathur and T. L. Dhama, *Nanoscale. Res. Lett.*, 2008, **3**, 444-453.
26. L. H. Teng and T. D. Tang, *J. Zhejiang. Univ-Sc. A*, 2008, **9**, 720-726.
27. C. Moreno-Castilla, M. V. Lopez-Ramon and F. Carrasco-Marin, *Carbon*, 2000, **38**, 1995-2001.
28. L. Wang, L. Ge, T. E. Rufford, J. L. Chen, W. Zhou, Z. H. Zhu and V. Rudolph, *Carbon*, 2011, **49**, 2022-2032.
29. J. Wei, R. Lv, N. Guo, H. G. Wang, X. Bai, A. Mathkar, F. Y. Kang, H. W. Zhu, K. L. Wang, D. H. Wu, R. Vajtai and P. M. Ajayan, *Nanotechnology*, 2012, **23**, 1-5.
30. L. Q. Hoa, M. C. Vestergaard, H. Yoshikawa, M. Saito and E. Tamiya, *J. Mater. Chem.*, 2012, **22**, 14705-14714.
31. A. R. Gliga, S. Skoglund, I. O. Wallinder, B. Fadeel and H. L. Karlsson, *Part. Fibre. Toxicol.*, 2014, **11**, 1-17.
32. F. B. Emilie Brun, Giulia Veronesi, Barbara Fayard, Stéphanie Sorieul, Corinne Chanéac, Christine Carapito, Thierry Rabilloud, Aloïse Mabondzo, Nathalie Herlin-Boime, Marie Carrière, *Part. Fibre. Toxicol.*, 2014, **11**, 1-16.
33. Y. T. Shieh, G. L. Liu, H. H. Wu and C. C. Lee, *Carbon*, 2007, **45**, 1880-1890.
34. R. B. Li, X. Wang, Z. X. Ji, B. B. Sun, H. Y. Zhang, C. H. Chang, S. J. Lin, H. Meng, Y. P. Liao, M. Y. Wang, Z. X. Li, A. A. Hwang, T. B. Song, R. Xu, Y. Yang, J. I. Zink, A. E. Nel and T. Xia, *ACS Nano*, 2013, **7**, 2352-2368.
35. C. M. Voge, J. Johns, M. Raghavan, M. D. Morris and J. P. Stegemann, *J. Biomed. Mater. Res. A*, 2013, **101A**, 231-238.
36. F. A. He and J. T. Fan, *Mater. Sci. Tech.-Lond*, 2013, **29**, 1423-1429.
37. S. H. Lecker, A. L. Goldberg and W. E. Mitch, *J. Am. Soc. Nephrol.*, 2006, **17**, 1807-1819.
38. C. O. Weill, S. Biri, A. Adib and P. Erbacher, *Cytotechnology*, 2008, **56**, 41-48.

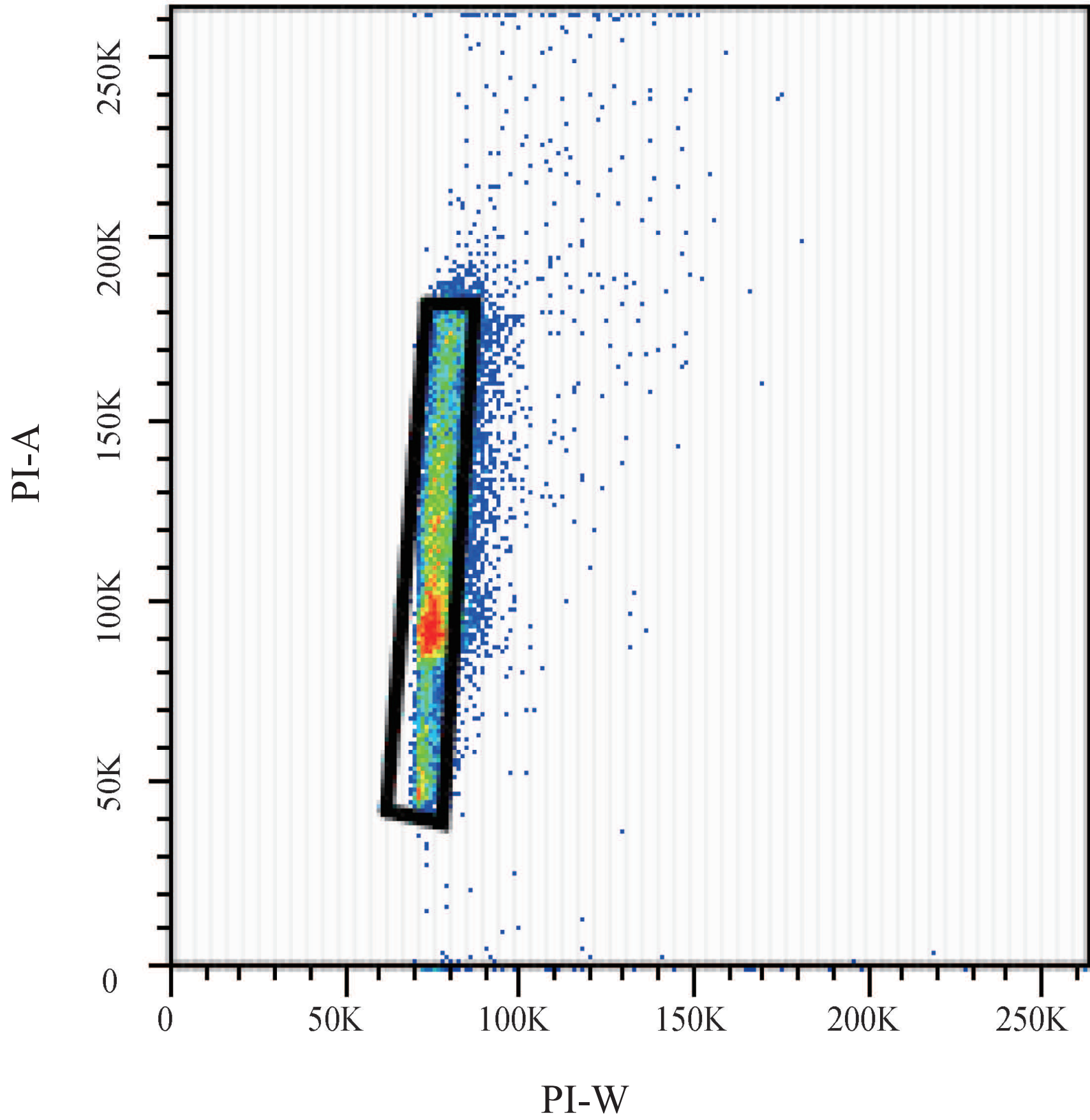
39. P. M. Martensen and J. Justesen, *Biotechniques*, 2001, **30**, 782-+.
40. T. Chen, J. J. Zang, H. F. Wang, H. Y. Nie, X. Wang, Z. L. Shen, S. C. Tang, J. L. Yang and G. Jia, *J. Nanosci. Nanotechnol.*, 2012, **12**, 8008-8016.
41. J. M. Worle-Knirsch, K. Pulskamp and H. F. Krug, *Nano Lett.*, 2006, **6**, 1261-1268.
42. X. Wang, J. Guo, T. Chen, H. Nie, H. Wang, J. Zang, X. Cui and G. Jia, *Toxicol. In Vitro*, 2012, **26**, 799-806.
43. J. J. Lemasters, A. L. Nieminen, T. Qian, L. C. Trost, S. P. Elmore, Y. Nishimura, R. A. Crowe, W. E. Cascio, C. A. Bradham, D. A. Brenner and B. Herman, *Bba-Bioenergetics*, 1998, **1366**, 177-196.
44. W. Zhong, X. Chen, P. Jiang, J. M. F. Wan, P. Qin and A. C. H. Yu, *Ultrasound Med. Biol.*, 2013, **39**, 2382-2392.
45. M. J. Berridge, *Cell. Signal. Bio.* 2012, **Module 1**, 1-63.
46. C. Bertoli, J. M. Skotheim and R. A. M. de Bruin, *Nat. Rev. Mol. Cell Bio.*, 2013, **14**, 518-528.
47. S. Bellucci, S. Dinicola, P. Coluccia, M. Bizzarri, A. Catizone, F. Micciulla, I. Sacco, G. Ricci and A. Cucina, *Int. Semiconduct. Con.*, 2012, **2**, 37-42.
48. D. Roxbury, X. M. Tu, M. Zheng and A. Jagota, *Langmuir*, 2011, **27**, 8282-8293.
49. L. Migliore, D. Saracino, A. Bonelli, R. Colognato, M. R. D'Errico, A. Magrini, A. Bergamaschi and E. Bergamaschi, *Environ. Mol. Mutagen.*, 2010, **51**, 294-303.
50. X. Q. He, S. H. Young, D. Schwegler-Berry, W. P. Chisholm, J. E. Fernback and Q. Ma, *Chem. Res. Toxicol.*, 2011, **24**, 2237-2248.
51. L. Rodriguez-Fernandez, R. Valiente, J. Gonzalez, J. C. Villegas and M. L. Fanarraga, *ACS Nano*, 2012, **6**, 6614-6625.
52. S. Kumar and V. Weaver, *Cancer Metast. Rev.*, 2009, **28**, 113-127.
53. S. E. Cross, Y. S. Jin, J. Rao and J. K. Gimzewski, *Nat. Nanotechnol.*, 2007, **2**, 780-783.
54. M. E. Dokukin, N. V. Guz and I. Sokolov, *Biophys J.*, 2013, **104**, 2123-2131.
55. J. Alcaraz, L. Buscemi, M. Grabulosa, X. Trepas, B. Fabry, R. Farre and D. Navajas, *Biophys J.*, 2003, **84**, 2071-2079.
56. J. Rheinlaender, N. A. Geisse, R. Proksch and T. E. Schaffer, *Langmuir*, 2011, **27**, 697-704.
57. Q. X. Mu, D. L. Broughton and B. Yan, *Nano Lett.*, 2009, **9**, 4370-4375.
58. M. Nikkhah, J. S. Strobl, E. M. Schmelz and M. Agah, *J. Biomech.*, 2011, **44**, 762-766.
59. M. W. Shen, S. H. Wang, X. Y. Shi, X. S. Chen, Q. G. Huang, E. J. Petersen, R. A. Pinto, J. R. Baker and W. J. Weber, *J. Phys. Chem. C.*, 2009, **113**, 3150-3156.

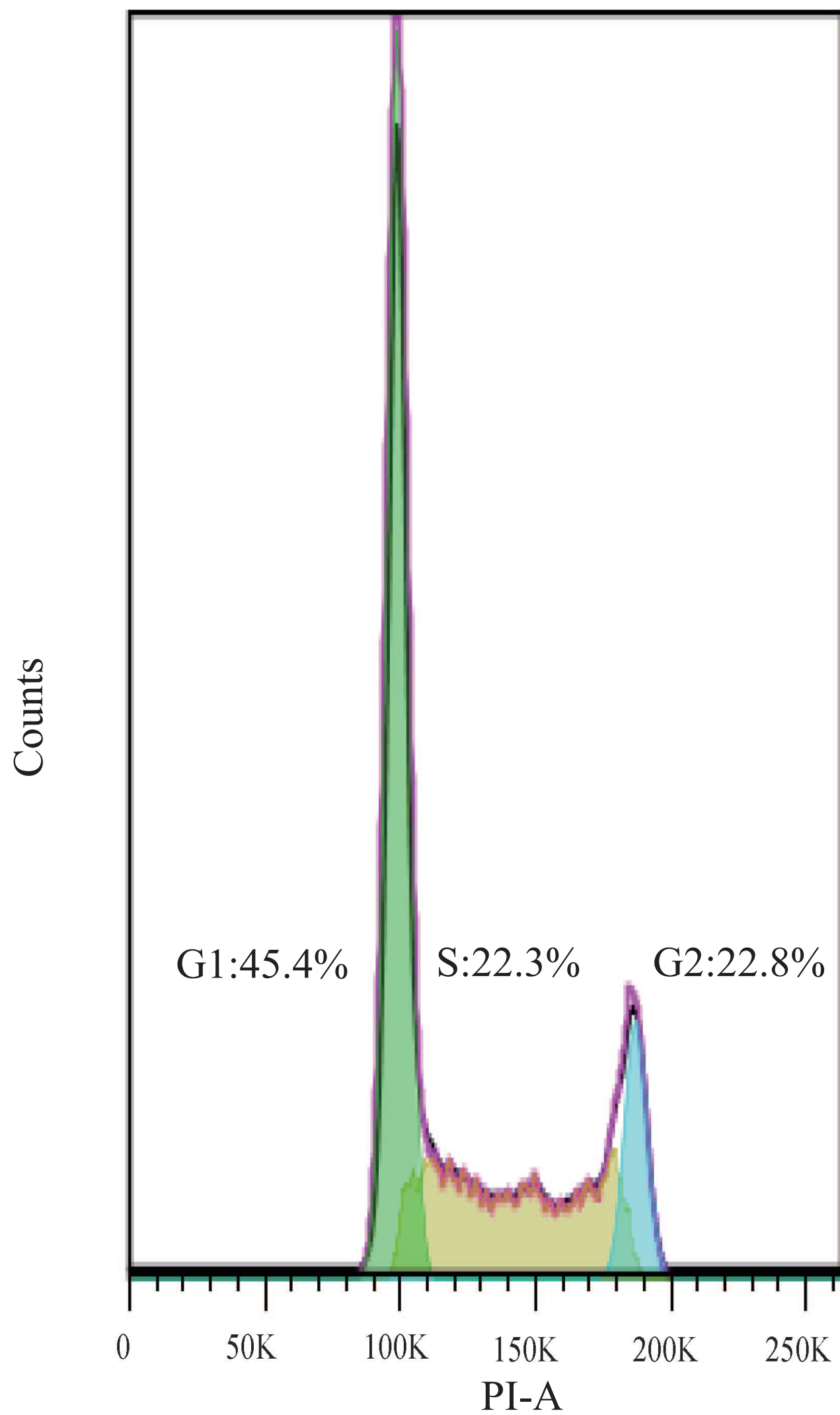


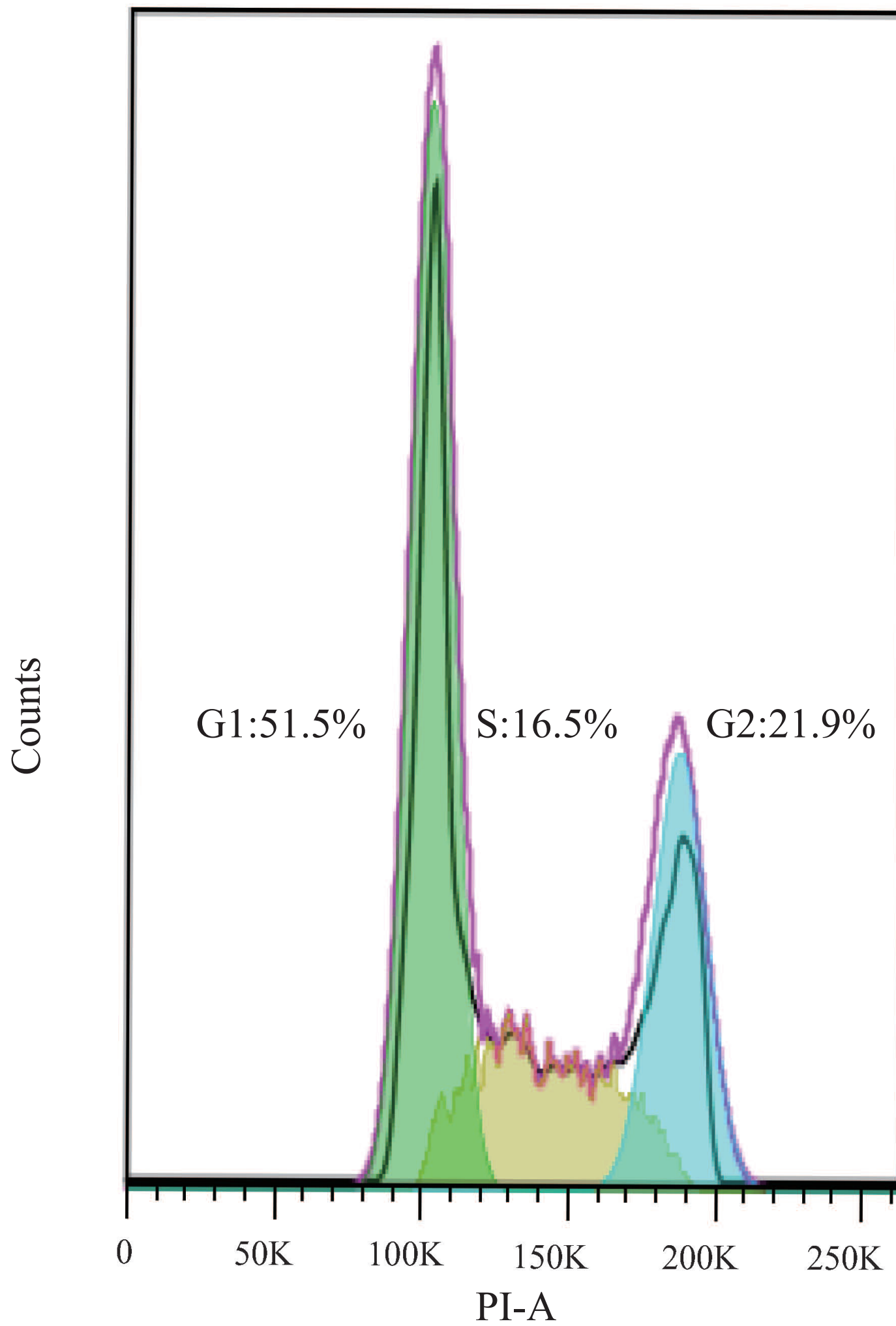


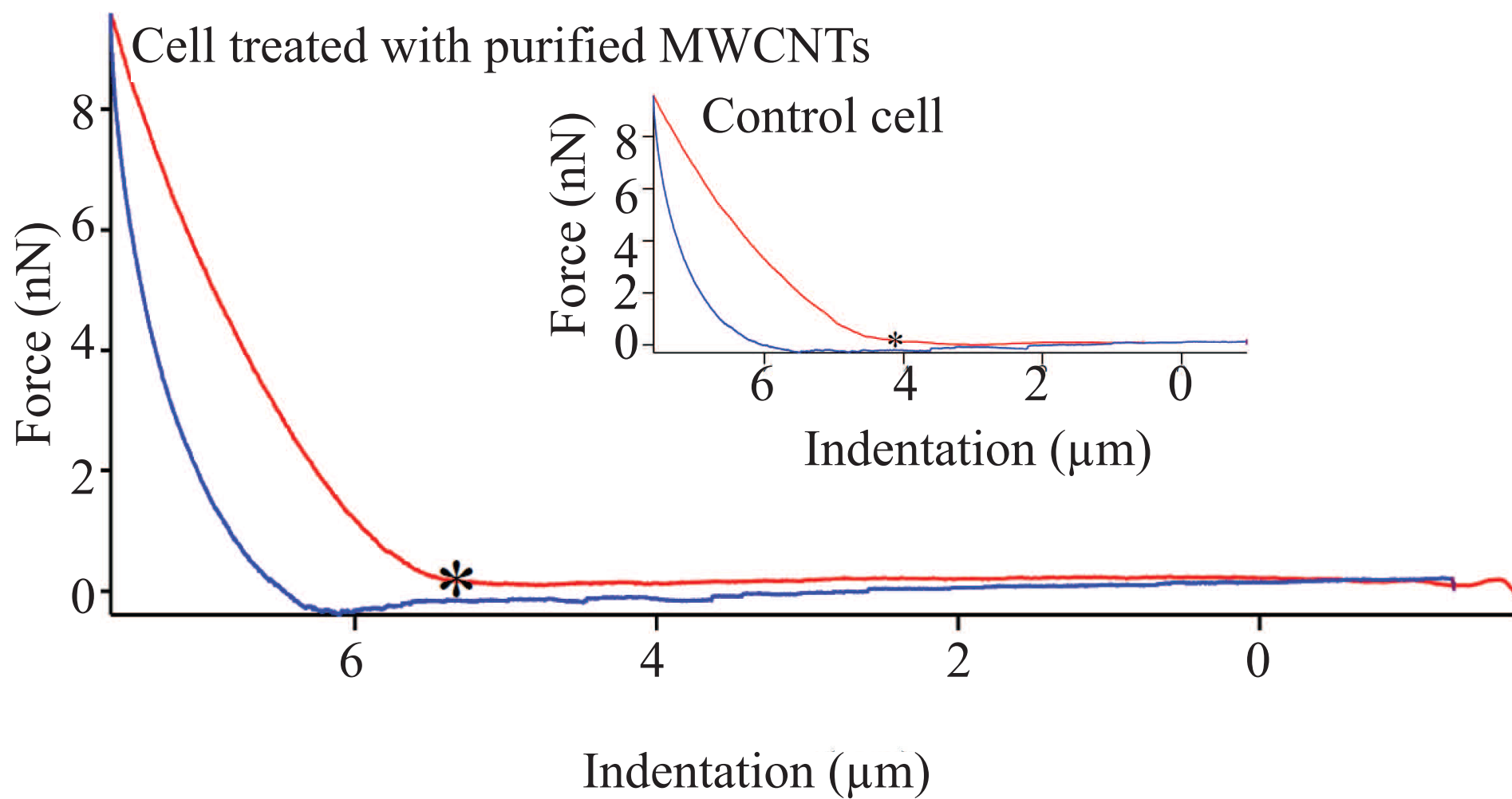
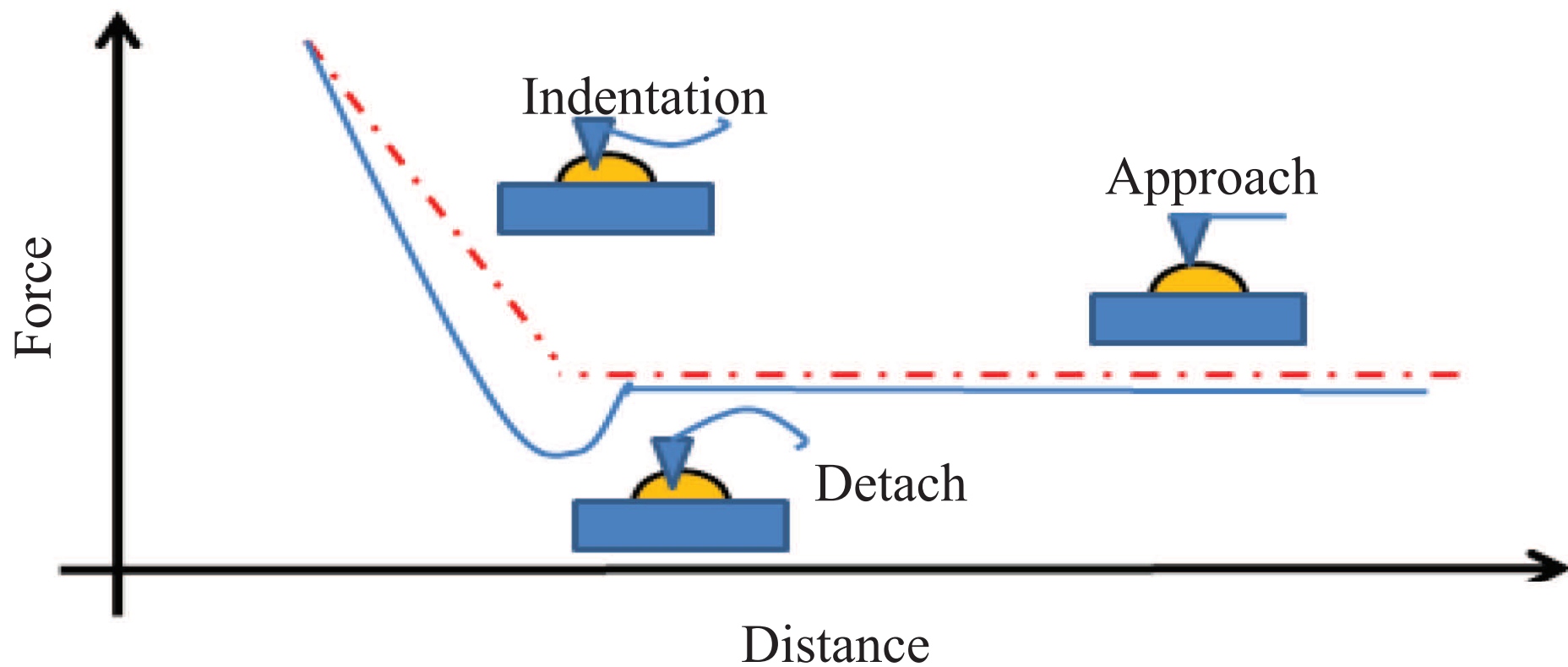


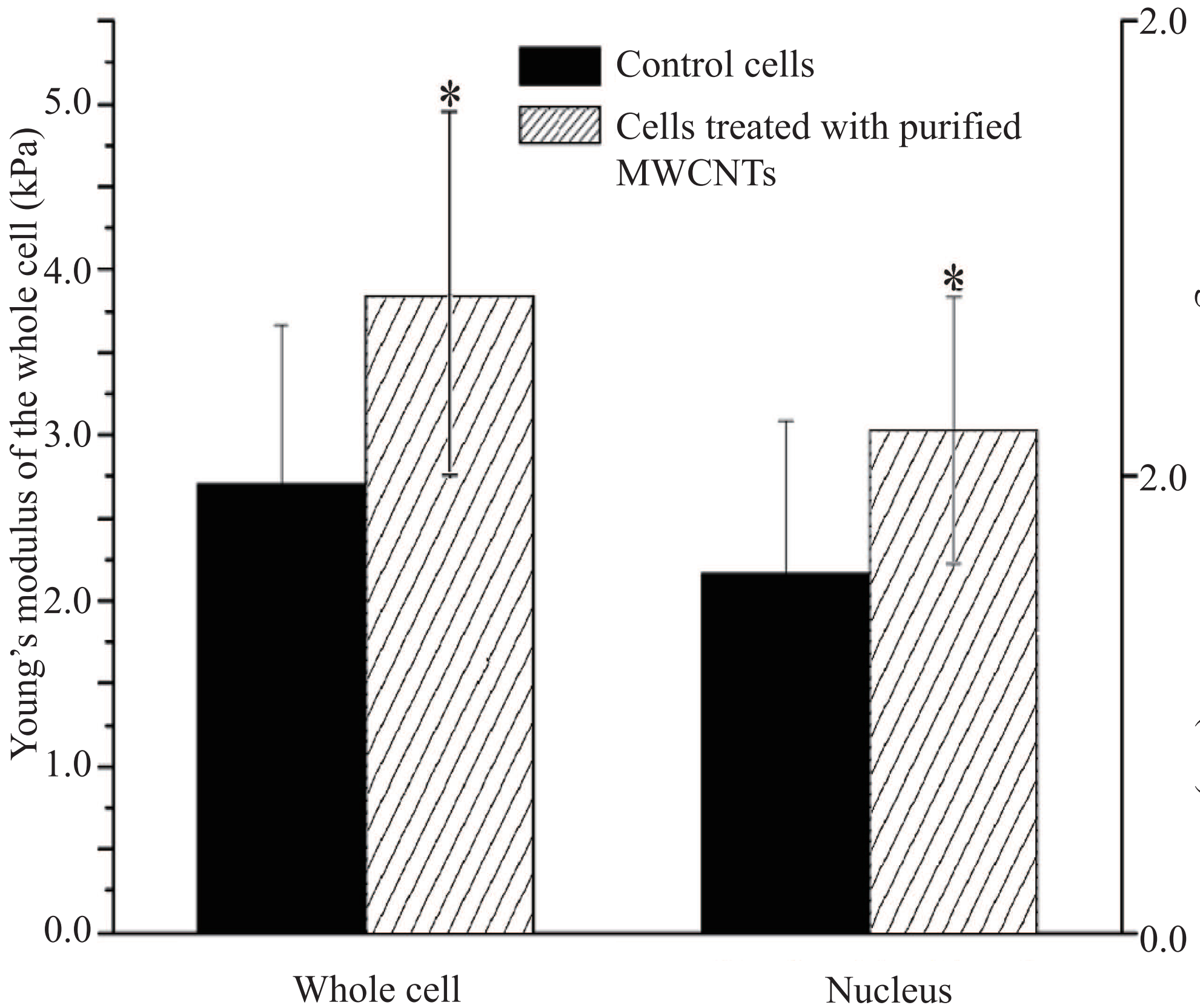












Environmental Science: Nano
MWCNTs

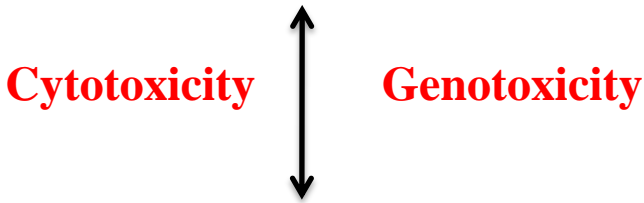
Physical and chemical
characterization



Human
bronchial
epithelial cells



Reduced mitochondrion activity
Cell cycle arrest
Changes in cellular
biomechanics



MWCNTs

Physical and chemical
characterization